Original Article

www.jmss.mui.ac.ir

Vesselness-guided Active Contour: A Coronary Vessel Extraction Method

Maryam Taghizadeh Dehkordi[1], Morteza Jalalat[1,2], Saeed Sadri[1], Alimohamad Doosthoseini[1], Mohammad Reza Ahmadzadeh[1], Rasoul Amirfattahi[1]

[1]Department of Electrical and Computer Engineering, Isfahan University of Technology, Isfahan, Iran, [2]Medical Image and Signal Processing Research Center, Isfahan University of Medical Sciences, Isfahan, Iran

Submission: 19-04-2013 Accepted: 05-01-2014

ABSTRACT

Vessel extraction is a critical task in clinical practice. In this paper, we propose a new approach for vessel extraction using an active contour model by defining a novel vesselness-based term, based on accurate analysis of the vessel structure in the image. To achieve the novel term, a simple and fast directional filter bank is proposed, which does not employ down sampling and resampling used in earlier versions of directional filter banks. The proposed model not only preserves the performance of the existing models on images with intensity inhomogeneity, but also overcomes their inability both to segment low contrast vessels and to omit non-vessel structures. Experimental results for synthetic images and coronary X-ray angiograms show desirable performance of our model.

Key words: *Active contour, vesselness-based, vessel extraction*

INTRODUCTION

Vessel extraction is a critical task in clinical practice. Correct assessment, especially accurate visualization and quantification of blood vessels traced in angiograms plays a significant role in a number of clinical diagnostic procedures, e.g. diagnosis relied on vessel width, reflectivity, tortuosity and abnormal branching. For example, appearance of vessels of a certain width in the heart may reveal the signs of stenoses. Grading of stenoses is of importance to diagnose the extent of vascular disease which determines the treatment therapy.[1,2] Although it is possible for medical experts to delineate vessels, but manual delineation of the vasculature becomes tedious or even impossible when the number of vessels in an image is large, or when a large number of images have to be inspected. Therefore, the development of automatic and accurate vessel-tree reconstruction from angiograms is highly desirable. In recent years, this has been a challenging task. The key fact is that vessels cannot be characterized uniformly. Since the blood, either by itself or by the contrast agent injected into it, is responsible for the vessel contrast to the background, vessels with larger widths usually have high contrast while smaller ones resemble the background. Many segmentation methods have been used to visualize the blood vessel structures in the human body. A review of vessel extraction techniques and algorithms can be found in.[3] A combination of Hessian matrix multi-scale filtering and region-growing is used to segment the coronary artery in angiograms.[4] An automatic technique, which provides correspondence between extracted vessels and pre-procedural vessels, improves the quality of disease diagnosis using multiple images and follow-up and provides important information for non-rigid image registration.[5] A segmentation method based on fusion algorithm is proposed in.[6] In this method, firstly, the coronary arteries are extracted by using the maximizing entropy segmentation method based on top-hat. Then the coronary arteries are extracted again by using the maximizing entropy segmentation method based on Gaussian filter. Finally, the last segmentation result is the image obtained by fusing two extracted coronary arteries images. A region-growing method is proposed for vessel segmentation in angiography images. The method consists of two parts: The feature map extraction based on a novel vesselness function; and the segmentation process which includes automatic seed-point selection, main branch segmentation and vessel detail repair. Both the greyscale and spatial information are extracted for segmentation based on region growing algorithm.[7] Furthermore, a classification approach is proposed to distinguish between the coronary arteries and background images using the shape context descriptor and the learning framework of spatial pyramid kernels.[8] In this paper, we focus on the new development of angiograms segmentation based on an active contour model.

Address for correspondence:
Mr. Morteza Jalalat, Department of Electrical and Computer Engineering, Isfahan University of Technology, Isfahan, Iran, Medical Image and Signal Processing Research Center, Isfahan University of Medical Sciences, Isfahan, Iran. E-mail: m.jalalat-evakilkandi@ec.iut.ac.ir

Active contour models are among the most successful image segmentation techniques in clinical applications. Active contours may be categorized as edge based[9-11] or region based.[12-15]

In region-based models, the statistical information inside and outside the contour are used to control the evolution. They are less sensitive to noise and are more effective for images with weak edges or images without edges. However, popular region-based active contour models[12,13] and[14] tend to rely on intensity homogeneity of each region to be segmented. For example, the popular piecewise constant models are based on the assumption that image intensities are statistically homogeneous (roughly constant) in each region.

In fact, intensity inhomogeneity often occurs in real images from different modalities. Generally for medical images, inhomogeneity is usually due to technical limitations or artifacts introduced by the object being imaged. In a study done by Li *et al*.,[16] Zhang *et al*.[17] and Wang *et al*.[18] proposed local binary fitting (LBF), local image fitting (LIF) and local Gaussian distribution (LGD) fitting models, respectively, capable to segment images with intensity inhomogeneity by embedding the local image information. When intensity inhomogeneity occurs in angiograms, each of these models can be used to segment the vessels. LIF model is more computationally efficient than LBF, but it cannot accurately extract vessels. Therefore, LBF model is more suitable for vessel segmentation in angiograms but it may fail to extract weak vessels.

In this paper, we propose a new approach for vessel extraction using LBF model by defining a novel vesselness-based term which segments low contrast vessels and omits non-vessel structures. The results are compared with the 4 active contour models.[12,16-18]

The remainder of this paper is organized as follows: In section 2, the LBF model is described. The proposed method is stated in section 3. Experimental results on synthetic images and real angiograms are presented in section 4 and section 5 is devoted to conclusion.

LBF MODEL

Let $\Omega \subset R^2$ be the image domain and I: $\Omega \to R$ be a given gray level image. To segment the images with intensity inhomogeneity, in[16] a region-based model using intensity information in local regions at a controllable scale is proposed. For an image, $I(x, y)$ on the image domain Ω, the algorithm proposes to minimize the following region-scalable fitting energy of a contour C:

$$F_1(C, f_1(P), f_2(P)) = \int_{\Omega} [\lambda_1 \int_{\Omega_1} K_\sigma(P-Q)|I(Q) - f_1(P)|^2 \, dQ + \lambda_2 \int_{\Omega_2} K_\sigma(P-Q)|I(Q) - f_2(P)|^2 \, dQ] \, dP \quad (1)$$

where, $P = (x, y)$, λ_1 and λ_2 are positive constants, C is the contour, $f_1(P)$ and $f_2(P)$ are two values that approximate image intensities in Ω_1 and Ω_2 (regions inside and outside the contour C, respectively), K_σ is a Gaussian kernel with a standard deviation σ. $I(Q)$ is the intensity of pixels in a window around P.

The energy in (1) is incorporated into a level set formulation. In the level set method, the curve $C \subset \Omega$ is represented by the zero level set of Lipschitz function ϕ: $\Omega \subset R$. Minimizing the energy functional F_1 with respect to ϕ using the gradient descent method leads to:

$$\frac{\partial \phi}{\partial t} = -\delta_\varepsilon(\phi)(\lambda_1 e_1 - \lambda_2 e_2) \quad (2)$$

Where e_1 and e_2 are the functions

$$e_i(P) = \int K_\sigma(Q-P)|I(P) - f_i(Q)|^2 \, dQ, \; i = 1, 2 \quad (3)$$

with

$$f_1(P) = \frac{K_\sigma(P) * [H_\varepsilon(\phi(P))I(P)]}{K_\sigma(P) * H\varepsilon(\phi(P))}$$
$$f_2(P) = \frac{K_\sigma(P) * [(1 - H_\varepsilon(\phi(P)))I(P)]}{K_\sigma(P) * (1 - H\varepsilon(\phi(P)))} \quad (4)$$

In practice, the Heaviside function in the above energy functional is approximated by a smooth function defined by

$$H_\varepsilon(x) = \frac{1}{2}\left[1 + \frac{2}{\pi}\arctan(\frac{x}{\varepsilon})\right] \quad (5)$$

Hence,

$$\delta_\varepsilon(x) = H'_\varepsilon(x) = \frac{1}{\pi}\frac{\varepsilon}{\varepsilon^2 + x^2} \quad (6)$$

As proposed in,[11] in order to maintain the regularity of the level set function a regularization term is incorporated into (2). Moreover, to regularize the zero level contour, the arc length term is also added to the energy function (2). After all, the level set evolution equation becomes:

$$\frac{\partial \phi}{\partial t} = -\delta_\varepsilon(\phi)((\lambda_1 e_1 - \lambda_2 e_2) + \upsilon(\nabla^2\phi - div(\frac{\nabla\phi}{|\nabla\phi|})) + \mu \, \delta_\varepsilon(\phi) div(\frac{\nabla\phi}{|\nabla\phi|}) \quad (7)$$

LBF model of (7) can well handle image with intensity inhomogeneity and is proper for angiograms segmentation.

Since the standard deviation, σ of the kernel controls the region-scalability,[16] for better results in angiograms, σ should be chosen according to size of vessels. In these images, a vessel tree is composed of two main parts:

The wide vessels and the thin ones. However in LBF model, only one scale parameter was used and hence that σ should be proportional to wide or thin vessels. If σ is appropriate for small vessels, it may cause undesirable results regarding low contrast vessels. Therefore, σ should be chosen proportional to wide vessels, making thin ones non-extractable. On the other hand, the statistical properties of these vessels also are different and the application of the model in (7) alone fails to extract all vessels. To address these problems, we add an energy term to LBF model as described in the following.

PROPOSED METHOD

Vesselness

In general, in the literature vessel enhancement in angiograms are Hessian-based filters, which are found to be sensitive to noise and sometimes give discontinued vessels due to junction suppression. To overcome these drawbacks, Truc *et al*.[19] proposed the use of line-like directional features of the image to obtain more precise Hessian analysis in noisy environments and to avoid junction suppression. The features are extracted by decimation-free directional filter bank (DDFB) which decomposed the input image to a set of directional images. Thus, it can correctly reveal small and thin vessels and yield the continuous vessel tree. Accordingly, in this paper we use this method to obtain enhanced image *D (Q)* needed in (10) except that we proposed a simple and fast method of the filter bank construction named fast directional filter bank (FDFB) presented in the following.

FDFB

In order to construct the directional filter bank (DFB) or DDFB,[19] it takes three stages. Through these stages, we have to modulate, down sample, resample and post-sample a pair of diamond-shaped like passband filters in DFB (or hourglass-shaped like passbands filters in DDFB). However in the FDFB directly and easily we partition the frequency domain using one stage division algorithm.

To achieve FDFB, we consider the frequency domain in polar co-ordinates as shown in Figure 1. It is supposed that the spectrum is divided into n parts, the i^{th} part is between $\theta_{i,min}$ and $\theta_{i,max}$ and the center of the i^{th} part is

$$\theta_i = \frac{\theta_{i,\min} + \theta_{i,\max}}{2} \tag{8}$$

A mathematical description of FDFB for 2^k DFBs is given by (9):

$$F_n = \begin{cases} 1, & \text{for} \begin{cases} \dfrac{(n-1)\pi}{2^k} \le \theta < \dfrac{n\pi}{2^k} \\ \forall r \text{ with } 0 \le u, v \le M \end{cases} \\ 0, & \textit{Otherwise} \end{cases} \tag{9}$$

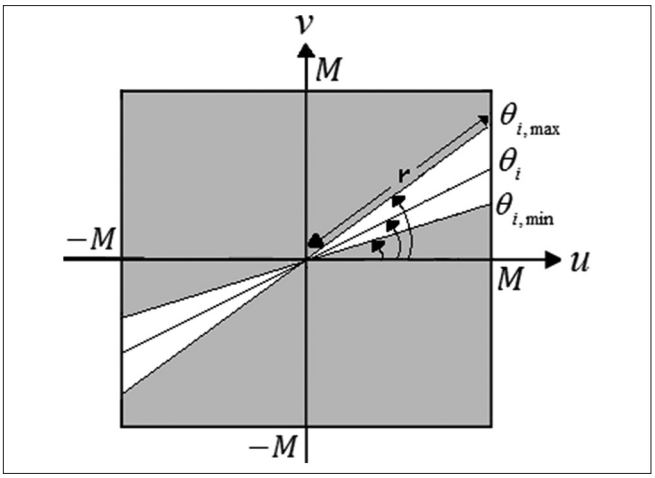

Figure 1: Consideration of frequency domain in polar coordinates

In which, u and v are frequency, $n \in \{1, 2,\ldots, 2^k\}$, $r = \sqrt{u^2 + v^2}$ and $\theta = \arctan(v/\upsilon)$. The ultimate partitioning of frequency domain in FDFB is equivalent to the output partitioning of DDFB, but it competes with less computational complexity.

One major problem with DDFB and FDFB is the inevitable ringing artifact. One way to remove ringing artifact is to smooth the filters transition band with a proper low pass Gaussian filter. Smoothed filter bank for $k = 3$ is shown in Figure 2. This filter bank partitions the frequency domain into eight sub-bands. In order to prevent aliasing, the input image is zero-padded to two times of its size. Since the angiographic images are square, we suppose the input image is $M \times M$. Hence, the frequency representation will be of the size $2M \times 2M$. The result of vessel enhancement in angiograms by Hessian-based filters is shown in Figure 3. As it demonstrates, some non-vessel parts of the image are enhanced.

Two-stage Level Set Formulation

Our method combines the two energy function based on (1) as:

$$F(C) = \alpha_I F_I(C, f_1, f_2) + \alpha_D F_D(C, d_1, d_2) \tag{10}$$

Where energies F_I and F_D are defined:

$$F_I(\phi, f_1, f_2) = \int \Big(\sum_{i=1}^{2} \lambda_i \int_{\Omega_i} K_{\sigma_0}(P-Q) I(Q) - f_1(P)\,|^2\, M_i^{\varepsilon}(\phi(Q))dQ\Big)dP \tag{11}$$

And

$$F_D(\phi, d_1, d_2) = \int \Big(\sum_{i=1}^{2} \lambda_{d_i} \int_{\Omega_i} K_{\sigma_1}(P-Q)\big|D(Q) - d_i(P)\big|^2\, M_i^{\varepsilon}(\phi(Q))dQ\Big)dP \tag{12}$$

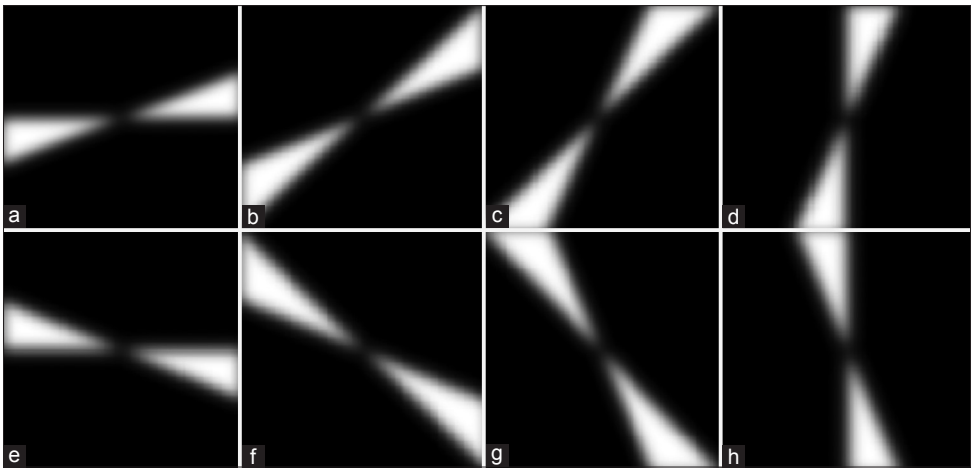

Figure 2: Partitioning of frequency domain, after smoothing filter is applied

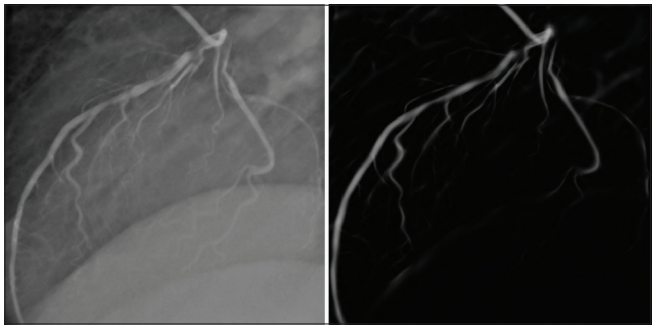

Figure 3: The result of vessel enhancement in angiograms by Hessian-based filters

In the first term of (10), *I (Q)* is the intensity of pixels in the original image and σ_0 is proportional to width of wide vessels. In the second term *D (Q)* is the intensity of pixels in enhanced image obtained by FDFB-based method (as presented in section 3.1) and includes the vessel structure. $d_1(P)$ and $d_2(P)$ are two values that approximate enhanced image intensities in Ω_1 and Ω_2 (regions inside and outside the contour *C*, respectively) and σ_1 is proportional to the width of thin vessels.

Finally, it is proposed to minimize the energy functional,

$$W(\phi) = \alpha_I(F_I(\phi, f_1, f_2) + \upsilon\vartheta(\phi)) + \alpha_D F_D(\phi, d_1, d_2) + \mu\rho(\phi) \quad (13)$$

Where α_I, α_D, υ, μ are regulating parameters and ρ (\varphi) is a level set regularization term as presented in[11]

$$\rho(\phi) = \int (|\nabla\phi(P)| - 1)^2 dP \quad (14)$$

Also, the arc length term is:

$$\vartheta(\phi) = \int_{\Omega} |\nabla H_\varepsilon(\phi(P))| dP \quad (15)$$

Let *H* be smoothed Heaviside function as defined in (5), then the proposed energy function *W (ϕ)* can be rewritten as (16)

$$\begin{aligned} W(\phi) = & \\ & \alpha_I[\int (\sum_{i=1}^{2} \lambda_i \int_{\Omega_i} K_{\sigma_0}(P-Q)|I(Q) - f_i(P)|^2 M_i^\varepsilon(\phi(Q))dQ)dP \\ & + \upsilon \int_{\Omega} \delta_\varepsilon(P)|\nabla\phi(P)|dP] + \mu \int \frac{1}{2}(|\nabla\phi(P)| - 1)^2 dP \\ & + \alpha_D[\int (\sum_{i=1}^{2} \lambda_{di} \int_{\Omega_i} K_{\sigma_1}(P-Q)|D(Q) - d_i(P)|^2 M_i^\varepsilon(\phi(Q))dQ)dP] \end{aligned} \quad (16)$$

where $M_1^\varepsilon(\phi) = H_\varepsilon(\phi)$, $M_2^\varepsilon(\phi) = 1 - H_\varepsilon(\phi)$.

According to[11] the functions $f_1(P)$ and $f_2(P)$ satisfy the following Euler–Lagrange equations:

$$\int K_{\sigma_0}(P-Q)M_i^\varepsilon(\phi(Q)(I(Q) - f_i(P))dQ = 0,\ i = 1.2 \quad (17)$$

From (17)

$$f_i(P) = \frac{K_{\sigma_0}(P) * [M_i^\varepsilon(\phi(P))I(P)]}{K_{\sigma_0}(P) * M_i^\varepsilon(\phi(P))},\ i = 1,2 \quad (18)$$

And $d_1(P)$ and $d_2(P)$ satisfy the following Euler–Lagrange equations:

$$\int K_{\sigma_1}(P-Q)M_i^\varepsilon(\phi(Q)(D(Q) - d_i(P))dQ = 0,\ i = 1, 2 \quad (19)$$

From (19):

$$d_i(P) = \frac{K_{\sigma_1}(P) * [M_i^\varepsilon(\phi(P))D(P)]}{K_{\sigma_1}(P) * M_i^\varepsilon(\phi(P))},\ i = 1, 2 \quad (20)$$

By keeping $f_1(P)$, $f_2(P)$ and $d_1(P)$, $d_1(P)$ fixed and minimizing the energy function *W (ϕ)*, the level set evolution equation becomes:

$$\frac{\partial \phi}{\partial t} = \delta_{\varepsilon}(\phi)\left\{\begin{array}{l}\alpha_I\left[\upsilon\ div(\frac{\nabla\phi}{|\nabla\phi|}) - (\lambda_1 e_1 - \lambda_2 e_2)\right] \\ \quad + \alpha_D\left[(\lambda_{d1} e_{d1} - \lambda_{d2} e_{d2})\right]\end{array}\right\} + \mu\ (\nabla^2\phi - div(\frac{\nabla\phi}{|\nabla\phi|})) \quad (21)$$

Where e_1 and e_2 are the functions

$$e_i(P) = \int K_{\sigma_0}(Q-P)\left|I(P) - f_i(Q)\right|^2 dQ,\ i = 1, 2 \quad (22)$$

e_{d_1} and e_{d_2} are the functions.

$$e_{d_i}(P) = \int K_{\sigma_1}(Q-P)\left|D(P) - d_i(Q)\right|^2 dQ,\ i = 1, 2 \quad (23)$$

IMPLEMENTATION AND EXPERIMENTAL RESULTS

Implementation

In a Core2 Duo CPU, 2.2 GHz and 4 GB RAM, it takes about 18 s for DDFB to create filter bank and for FDFB it takes about 3 s.

In our approach, the level set function (21) was evaluated in two stages. In the first stage, in order to propagate the contour to the main vessels, α_I, α_D are set to one and zero, respectively and $\lambda_1 = \lambda_2 = 1$, $\mu = 1$, $\upsilon = 65$, $\Delta t = 0.1$, the same as.[16] In the second stage to segment thin vessels, α_I, α_D are set to zero and 1, respectively and $\lambda_{d1} = \lambda_{d2} = 1$. It should be mentioned that the second stage is only effective in the narrowband case.

In the first term of (21), σ_0 is selected according to the width of main vessels and in the second term, σ_1 is selected proportional to width of thinner vessels. For angiograms $\sigma_0 = 3$, $\sigma_1 = 1$ is desirable.

RESULTS

To evaluate the result of the proposed algorithm for vessel segmentation in angiograms, it has been tested with synthetic and real images.

Figure 4 shows two synthetic images corrupted by intensity inhomogeneity. The image in Figure 4a is a synthetic image convolved with a Gaussian function to model the real angiogram. The results of the original image segmentation by LBF model and our method are shown in Figure 4b and c, respectively.

The image in Figure 4d is generated by adding Gaussian noise with $\sigma = 0.005$ to Figure 4a. The segmentation result for noisy image by LBF model and our method are shown at Figure 4e and f, respectively.

It is apparent that our algorithm segments the vessels more precisely than LBF in noisy images. Also, the results of our algorithm for the original image and the image with a high level of noise are very close as shown in Figure 4e.

Figure 5 compares the performance of our proposed algorithm on two real coronary X-ray angiograms. In the left most column, the original images are of size 300 × 300. The second and third columns show the results of converged contour of LBF and our method for real coronary X-ray angiograms. The fourth and fifth columns show the results of segmentation of LBF and proposed method respectively. It is clear that our algorithm has been able to extract vessels with weak boundaries more precisely. In addition, our algorithm demonstrates the width of the main vessels more accurate than that of LBF.

As shown in Figure 6, the results of LBF and our method on another angiogram are shown. Our method extracts the vessels in angiograms with a complex background and noise, accurately.

In order to compare our results with the results of the four above mentioned active contour models, we randomly selected 15 X-ray coronary angiograms obtained in Sina Heart Hospital, Isfahan, Iran. These images were segmented manually by an expert at this center as a gold standard.

For performance comparison, we have selected the segmentation accuracy (ACC) measure, determined by true positive fraction (TPF) and the false positive fraction (FPF). The parameter TPF, also called "sensitivity," is the ratio of the number of pixels correctly classified as vessel pixels true positive (TP), to the total number of vessel pixels in the gold standard segmentation,

$$\text{TPF} = \frac{\text{TP}}{\text{P}} = \frac{\text{TP}}{\text{TP}+\text{FN}} = \text{sensitivity}$$

where FN is the number of pixels incorrectly classified as non-vessel pixels. The ideal amount of TPF is equal to 1.The parameter FPF is the number of pixels incorrectly classified as vessel pixels false positive, divided by the total number of non-vessel pixels in the gold standard:

$$\text{FPF} = \frac{\text{FP}}{\text{N}} = \frac{\text{FP}}{\text{FP}+\text{TN}} = 1\text{-specificity}$$

Here, TN is the number of pixels correctly classified as non-vessel pixels. The ideal amount of TPF is equal to 0. The ACC for one image is the ratio of the total number of correctly classified points (sum of TPs and true negatives) by the total number of points in the image.

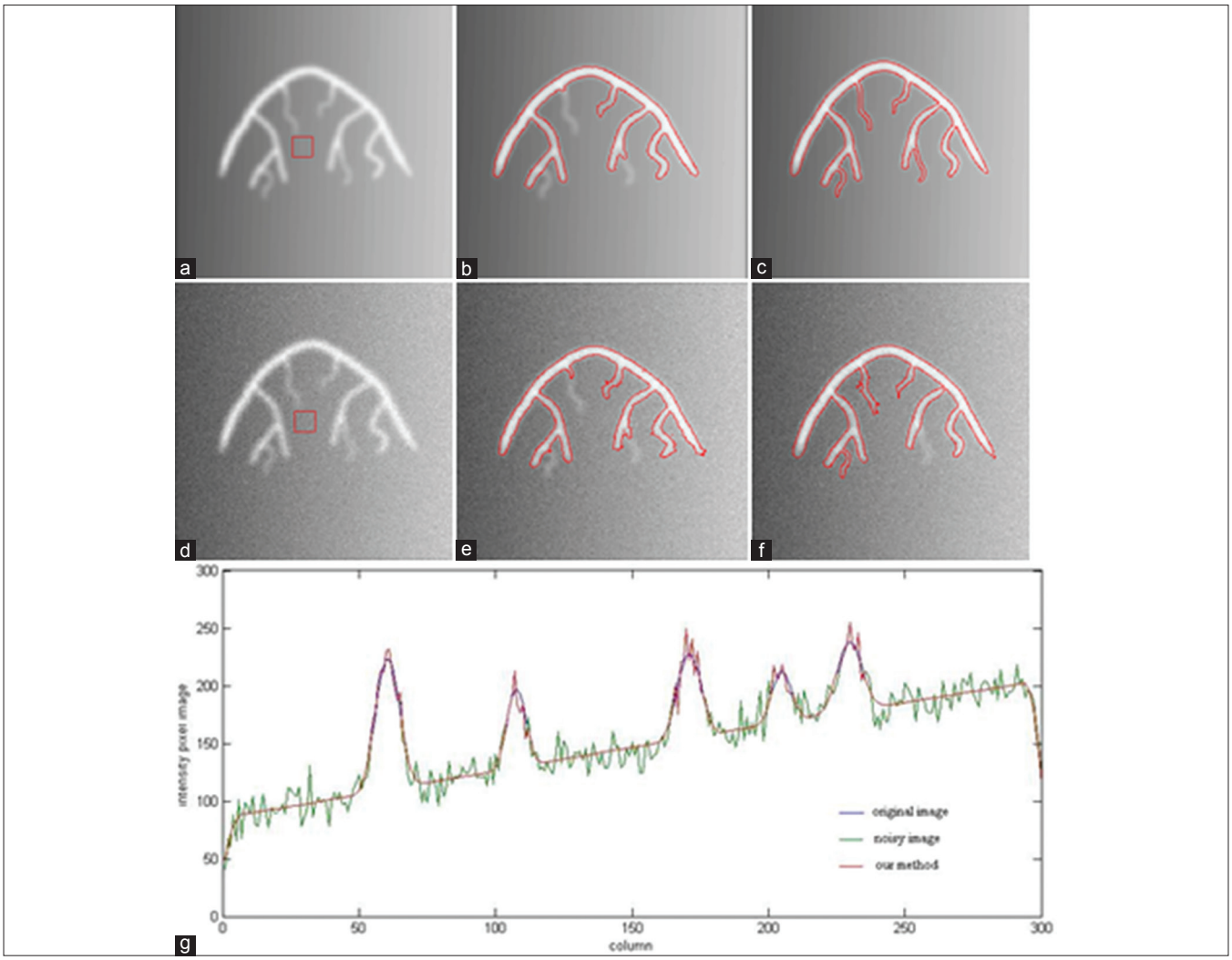

Figure 4: The results of local binary fitting (LBF) and our method on synthetic image with and without noise: (a and d) Initial contour and the original image (b and c) Final contour of clean image by LBF model and our method, respectively (e and f) Final contour of noisy image by LBF model and our method, respectively (g) Cross-section of the original image (blue line), noisy image (green line) and our method (red line)

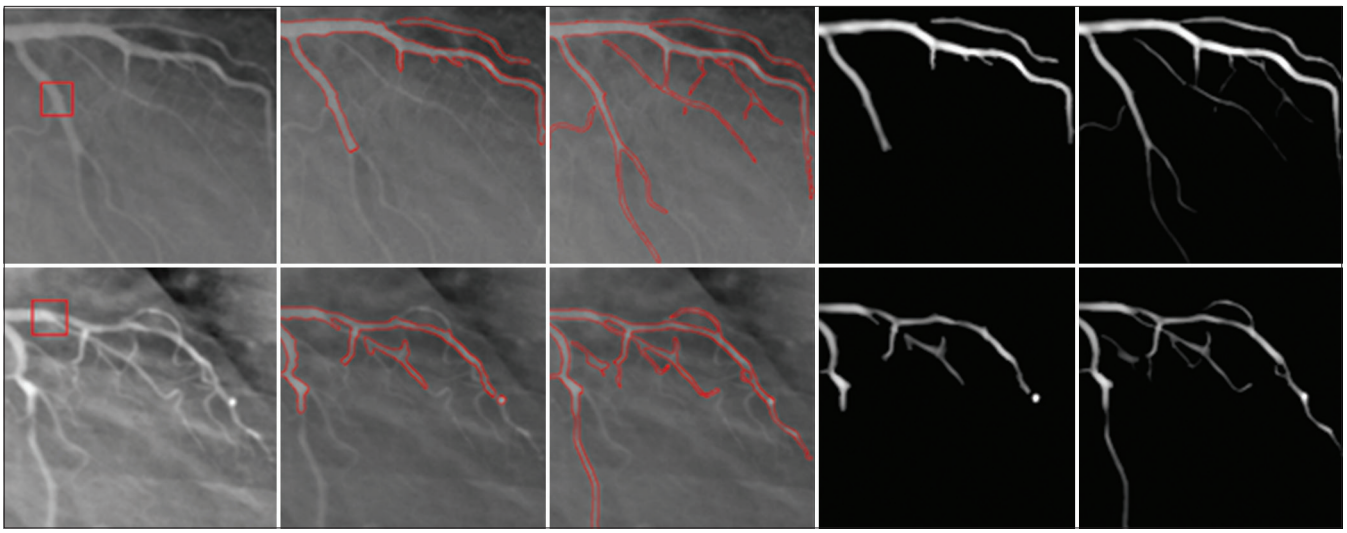

Figure 5: The results of local binary fitting (LBF) model and our method for coronary X-ray angiograms. Original images and initial contours (first column), final contour by LBF method (second column), our method (third column), segmentation result by LBF method (forth column) and by our method (fifth column)

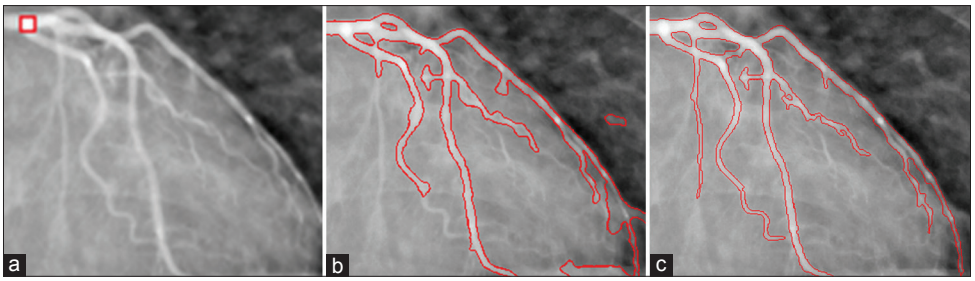

Figure 6: The results of local binary fitting (LBF) and our method on an angiogram. (a) Original image and initial contour. (b) LBF. (c) Our method

Table 1: Performance of vessel segmentation by active contour methods

	True positive fraction	False positive fraction	Accuracy (standard deviation)
Our method	0.8943	0.012	0.9747 (0.0085)
LBF[11]	0.8127	0.018	0.9053 (0.0102)
LIF[12]	0.1812	0.008	0.7524 (0.0072)
LGD[13]	0.3012	0.025	0.8471 (0.0192)
Chan and Vese[7]	0.1732	0.2326	0.6596 (0.0135)

LBF – Local binary fitting; LIF – Local image fitting; LGD – Local Gaussian distribution

$$ACC=\frac{TP+TN}{P+N}=\frac{TP+TN}{TP+FN+FP+TN}$$

The ideal amount of ACC is also equal to 1.

Table 1 shows the average of the ACC measurements for all 15 angiograms for our method, LBF, LIF, LGD and Chan-Vese models. It is apparent that the performance of our method is better than the other methods.

CONCLUSIONS

In this paper, we have presented a new active contour model for vessel segmentation presented in (21). In the level set formulation, the new approach combines both intensity information in regions with a controllable scale and information of the image enhanced by FDFB-based method. The first term in (21) extracts the main vessels using LBF model, by incorporating the vessel structure while the second term extracts thin vessels. Applying LBF model alone fails to extract all vessels. Also, if the first term is omitted, the vesselness-based term might segment non-vessel structures. Therefore, a combination of the two terms leads to a better result than using each term alone. The model is efficient for the segmentation of vessels as well as other line-like structures. In conclusion, the proposed method is a more accurate candidate for segmentation coronary vessels used in clinical tasks.

ACKNOWLEDGMENTS

The authors wish to thank Dr. Mohammad Hashemi of Sina Heart Hospital, Isfahan, Iran for his helps and Dr. Li Wang for making source code of LGD model available to use. This work is part of a research project supported by Medical Image and Signal Processing Research Center, Isfahan University of Medical Science, Isfahan.

REFERENCES

1. North American Symptomatic Carotid Endarterectomy Trial. Methods, patient characteristics, and progress. Stroke 1991;22:711-20.
2. Randomised trial of endarterectomy for recently symptomatic carotid stenosis: Final results of the MRC European Carotid Surgery Trial (ECST) Lancet 1998;351:1379-87.
3. Kirbas C, Quek F. A review of vessel extraction techniques and algorithms. ACM Comput Surv 2004;36:81-121.
4. Wang S, Li B, Zhou S. A segmentation method of coronary angiograms based on multi-scale filtering and region-growing. Biomedical Engineering and Biotechnology (iCBEB), International Conference on. IEEE, 2012. p. 678-81.
5. Huang X, Zaheer S, Abdalbari A, Looi T, Ren J, Drake J. Extraction of liver vessel centerlines under guidance of patient-specific models. In: Engineering in Medicine and Biology Society (EMBC), 2012 Annual International Conf of the IEEE. 2012. p. 2347-50.
6. Kang WW, Kang XT, Liu B. The segmentation method based on fusion algorithm of transition region extraction for coronary angiograms. Adv Mater Res 2012;542-3:616-9.
7. Li Y, Zhou S, Wu J, Ma X, Peng K. A novel method of vessel segmentation for X-ray coronary angiography images. In: Computational and Information Sciences (ICCIS), 2012 Fourth International Conference on, 2012. p. 468-71.
8. Wang F, Zhang Y, Greenspan H, Syeda-Mahmood T, Beymer D. Automatic classification of images of an angiography sequence using modified shape context-based spatial pyramid kernels. In: Biomedical Imaging: From Nano to Macro, 2011 IEEE International Symposium on, 2011. p. 1091-6.
9. Caselles V, Kimmel R, Sapiro G. Geodesic active contours. Int J Comput Vis 1997;22:61-79.
10. Xiang Y, Chung AC, Ye J. An active contour model for image segmentation based on elastic interaction. J Comput Phys 2006;219:455-76.
11. Li C, Xu C, Gui C, Fox MD. Level set evolution without re-initialization: A new variational formulation. In: Proc. IEEE Conf. Computer Vision and Pattern Recognition, CVPR, Vol. 1. 2005. p. 430-6.
12. Chan T, Vese L. Active contours without edges. IEEE Trans Image Process 2001;10:266-77.
13. Paragios N, Deriche R. Geodesic active regions and level set methods for supervised texture segmentation. Int J Comput Vis 2002;46:223-47.
14. Xie X, Mirmehdi M. MAC: Magnetostatic active contour model. IEEE Trans Pattern Anal Mach Intell 2008;30:632-46.
15. Lie J, Lysaker M, Tai XC. A binary level set model and some applications to Mumford-Shah image segmentation. IEEE Trans Image Process 2006;15:1171-81.
16. Li C, Kao CY, Gore JC, Ding Z. Minimization of region-scalable fitting energy for image segmentation. IEEE Trans Image Process

2008;17:1940-9.
17. Zhanga K, Song H, Zhang L. Active contours driven by local image fitting energy. Pattern Recognit 2010;43:1199-206.
18. Wang L, He L, Mishra A, Li C. Active contours driven by local Gaussian distribution fitting energy. Signal Process Vis Inf Anal Secur 2009;89:2435-447.
19. Truc PT, Khan MA, Lee YK, Lee S, Kim TS. Vessel enhancement filter using directional filter bank. Comput Vis Image Underst 2009;113:101-12.

How to cite this article: Dehkordi MT, Jalalat M, Sadri S, Doosthoseini A, Ahmadzadeh MR, Amirfattahi R. Vesselness-guided active contour: A coronary vessel extraction method. J Med Sign Sens 2014;4:150-7.

Source of Support: This work is part of a research project supported by Medical Image and Signal Processing Research Center, Isfahan University of Medical Science, Isfahan, **Conflict of Interest:** None declared

BIOGRAPHIES

Maryam Taghizadeh Dehkordi received the B.Sc. degree in electrical engineering from the Isfahan University of Technology, Isfahan, Iran, in 2001. She received the M.Sc. and PhD degree in communication engineering in 2004 and 2014, respectively from the Isfahan University of Technology, Isfahan, Iran. Her main fields of interest include image processing.

E-mail: maryam_td121@yahoo.com

Morteza Jalalat received the B.Sc. degree in electrical engineering from the Tabriz Azad University, Tabriz, Iran, in 2008. He received the M.Sc. degree in communication engineering in 2011 from the Isfahan University of Technology, Isfahan, Iran. His main fields of interest include computer vision and digital signal processing.

E-mail: m.jalalat-evakilkandi@ec.iut.ac.ir

Saeed Sadri Associate Professor in Electrical and Computers Engineering Department, Isfahan University of technology, Isfahan, Iran. He received the B.Sc. and the M.Sc. degree in electrical engineering from the University of Tehran, Faculty of Engineering, Tehran, Iran, respectively in 1977 and 1979. He eceived the PhD degree in communication engineering from the Isfahan University of Technology, in 1997.

E-mail: sadri@cc.iut.ac.ir

Alimohamad Doosthoseini Associate Professor in Electrical and Computers Engineering Department, Isfahan University of technology, Isfahan, Iran. He received the B.Sc. degree in communication engineering from the Shiraz University, Shiraz, Iran, in 1975. He received the M.Sc. degree in communication engineering from the University of California, Berkeley, California, USA, in 1977. He received the PhD degree in communication engineering from the Stanford University, California, USA, in 1983.

E-mail: alimdh@cc.iut.ac.ir

Mohammad Reza Ahmadzadeh received his BSc degree in Electronic Engineering from the Ferdowsi University of Mashhad, Iran in 1989 and the MSc degree in Electronic Engineering from the University of Tarbiat Modarres, Tehran in 1992. He received his PhD from University of Surrey, UK in 2001. He was a lecturer at Shiraz University from 1993-1997, and an Assistant Professor from 2001-2004. He is an Assistant Professor of Electrical Engineering at Isfahan University of Technology, Iran from 2004. His research interests include image processing, pattern recognition, reasoning with uncertainty, expert systems, information fusion and neural networks.

E-mail: ahmadzadeh@cc.iut.ac.ir

Rasoul Amirfattahi was born in 1969. He received BS degree in Electrical Engineering from Isfahan University of technology, Isfahan, Iran in 1993, MS degree in Biomedical Engineering and Ph.D degree in Electrical Engineering both from Amirkabir University of technology (The Tehran Polytechnic), Tehran, Iran in 1996 and 2002 respectively. From 2003 he joined Isfahan University of Technology while he is currently an Associate Professor and director of digital signal processing research laboratory at department of Electrical and Computer Engineering. His research interests include Biomedical signal and image processing, speech and audio analysis, Biological system modeling and DSP algorithms. He is an author or coauthor of more than 150 technical papers, one book and two book chapters.

E-mail: fattahi@cc.iut.ac.ir